

Performance of a flanged diffuser augmented wind turbine structure with and without the presence of the turbine: 3D Study

Amr M. Abdelrazek^{(1).(*)}, Amira M. Abdelrazik⁽²⁾, Sadek Z. Kassab⁽²⁾

Abstract

In the present study, a structure consisting of a nozzle, a diffuser and a flange was constructed and modeled using a 3-dimensional, 3D, model using ANSYS-FLUENT 6.3. The aim of this study is to get the results for an optimum geometric shape that generates the highest wind velocity in front of the wind turbine installed inside the structure at the position where the air velocity is maximum. In addition, another aim of the study is to compare the results of the 3D model in case of the presence of the wind turbine inside the flanged diffuser augmented wind turbine, FDAWT, structure with the case of empty structure (without the turbine). The obtained 3D model results for velocity and pressure distributions within the study domain are compared with the results obtained previously by the present authors using 2D model.

The present 3D study reveals that: The maximum velocity along the structure centerline at the throat of the FDAWT structure is increased by 70% before inserting the turbine. This value decreases to 63% after inserting the turbine, compared to 71% increase for the case of 2D modeling obtained by the present authors in previous studies. There is no change in the trends of the velocity and pressure distributions for the three cases.

Keywords: Wind turbine, flanged diffuser, 3D, CFD

1- Introduction

In recent years, the world realized that the supply of fossil fuels is limited; this has sparked a fire to search for other ways to keep up with the increasing demand for energy. Now days there are two new major types of energy sources, the nuclear and the renewable energy sources. The focus of the present study is in the renewable energy, more specifically wind energy. In addition, the present study focuses on how to make the smaller wind turbine suitable to the urban areas characterized by low wind speed.

The power in wind, P, is well known to be proportional to the cubic power of the wind velocity, V_∞ approaching the wind turbine.

$$P = \frac{1}{2} \rho V_\infty^3 C_p A \quad (1)$$

Where: ρ is the air density, C_p is the power coefficient, and A is the rotor swept area.

This means that even a slight increase in wind velocity gives a large increase in energy output. Therefore, many studies tried to find a way to increase the wind velocity. Some of these studies adopt a diffuser-shaped structure surrounding the wind turbine, the other adopt a flange attached at the exit of diffuser shroud.

A wind energy system that significantly reduces the cost of energy has long been sought. The Diffuser Augmented Wind Turbine (DAWT) is thought to provide such an opportunity. The idea is surrounding a wind turbine rotor with a duct. A large flange is attached to the outer periphery of a duct exit. This flange produces a low-pressure region to create separation behind it to collect and accelerate more wind and increase the wind velocity inside the structure compared to a diffuser with no flange.

The flanged diffuser augmented wind turbine (FDAWT) concept is explored from its origins, as one of a number of alternative wind energy systems, through the development of the DAWT. The FDAWT presents a significant advancement in the reduction of cost of energy for the augmented wind turbine concept, Olivieri [1].

(1) Eng. Mathematics and Physics Dept, Faculty of Engineering, Alexandria University, Egypt,

Corresponding author

(2) Mechanical Eng. Dept., Faculty of Engineering, Alexandria University, Egypt,

De Vries [2] has a first trial to improve theory for DAWT. He characterizes simple diffuser theory from shrouded turbine theory. In the simple diffuser theory, De Vries models the one dimensional, 1D, flow through the diffuser, but noticed that the exit pressure should be equal to atmospheric pressure.

Ohya et al. [3] discovered that a wind turbine system was developed that consists of a diffuser shroud with a broad-ring flange at the exit periphery of the diffuser. The flange plays a major role in accelerating the approaching wind velocity and it also replaces the need of yaw control mechanism. Sarwar et al. [4] developed a new diffuser augmented wind turbine system with a flange at the exit periphery. Results were analyzed from the experimental setup and came to know that wind speed in the diffuser was greatly affected by the diffuser open angle, flange height, center body length, inlet shape, and hub ratio. As a result, the power augmentation was remarkably increased by a factor of 2.5.

Jafari and kosasih [5] pointed out that, CFD simulations have been carried out on a small commercial wind turbine with a simple frustum diffuser shrouding. The results showed that these parameters play a prominent role in sub-atmospheric back pressure and flow separation in the diffuser. Hjort and Larsen [6] presented a new system of diffuser augmented wind turbines (DAWTs). The one-dimensional momentum theory which governing the DAWT is studied, and presented the power extraction restrictions applies for a Horizontal Axis Wind Turbine, HAWT, to push the diffuser design to high power coefficients.

The inner flow of three hollow structures was examined, a nozzle-type, a cylindrical-type model and a diffuser-type. Ohya et al. [3]. The results show the wind velocity distribution, U/U_∞ , and pressure coefficient distribution, C_p , on the central axis of a hollow-structure model. The diffuser model has the highest velocity ratio $U/U_\infty \approx 1.8$ and the lowest pressure coefficient value at the diffuser throat $X/L = 0$. This means that the diffuser structure has the best effect on collecting and accelerating the wind.

As a result of many trials, it is concluded that the velocity is increased when adding an inlet nozzle and a ring type flange to the diffuser exit. The inlet shroud is a curved surface surrounding the diffuser model inlet. The flange is added vertically to the diffuser model exit, Fig. 1. By adding the inlet shroud and the flange, a great raise in the wind velocity can be obtained, better than the case of diffuser model only, Ohya et al. [3] and Abe et al. [7].

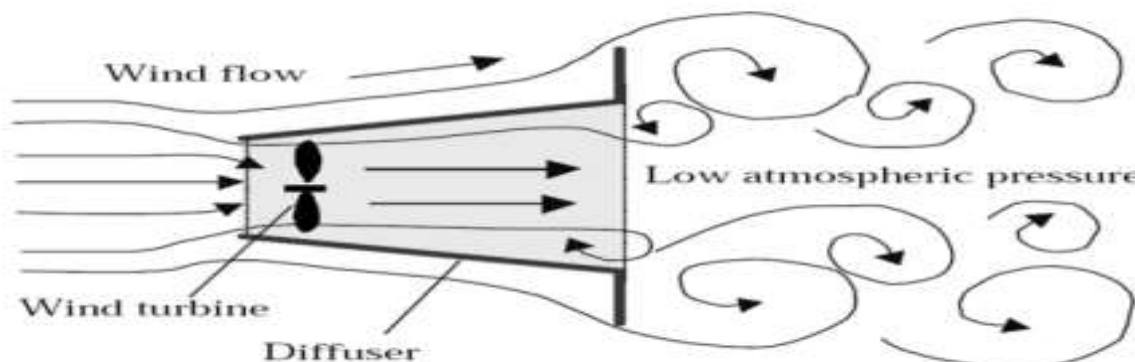


Figure 1 Schematic cross-sectional view of a diffuser and wind speed increase mechanism, Abe et al. [7].

The using of a flanged diffuser produces a great increase in the output power coefficient, C_w , nearly 5 times that of a standard wind turbine is reached. The experimental results were obtained under the same wind speed and swept area of a wind turbine, Ohya et al. [3].

Abdulaziz [8] performed an optimization study by carrying out numerical investigations for the air flow inside a flanged diffuser augmented wind turbine structure using the ANSYS Fluent CFD software. He concluded that, the best geometric shape of the flanged diffuser, where the results selection was based on the generation of the highest wind velocity inside the flanged diffuser. The results proved that a flanged diffuser equipped with a nozzle angle of 26° , nozzle length of $0.2D$, flange length of $0.9D$, diffuser angle of 20° , diffuser length of $1.35D$ and a flange angle of 90° are the optimum values, where D is the diffuser throat diameter. Abdulaziz performed his study by changing only one parameter and keep the other four parameters constant. This way of study raised the problem of the effect of the parameters arrangement on the obtained results.

Abdelrazik [9] performed a CFD study in order to find an optimum shape for flanged diffuser augmented wind turbine (FDAWT) Structure. Nozzle length, nozzle angle, diffuser length, diffuser angle and flange height are the parameters used to

represent the performance of the FDAWT. She used design of experiments technique to get several combinations of these five parameters. The flow velocity predicted by the simulation is analyzed through two different regression models, with and without interaction terms, according to multi-linear regression using LU decomposition to solve a system of algebraic equations. These models are validated by comparing the results with the obtained CFD results.

While, Abdelrazek et al. [10] are numerically studied the variations in the performance of a flanged diffuser augmented wind turbine (FDAWT) structure working under variable geometrical conditions. Nozzle angle, nozzle length, diffuser angle, diffuser length, and flange height are the five parameters chosen to control the performance of the FDAWT structure. Thirty random cases are studied numerically using ANSYS FLUENT6.3. The velocity and pressure distributions and contours are presented. The effect of each parameter on the performance of FDAWT structure is presented and discussed. They concluded that the velocity ratio of the maximum air velocity along the structure axis, V_{max} , and the wind velocity, V_0 , V_{max}/V_0 , reaches a maximum value $V_{max}/V_0 = 1.83$ and a minimum value $V_{max}/V_0 = 1.3$. Between these two values there is no observed trend for the results of the 30 random cases.

Finally, recent reviews for the flanged diffuser augmented wind turbine (FDAWT) structure can be found in Abdulaziz [8], Abdelrazik [9] and Abdelrazek et al. [10].

In the present study, a structure consists of a nozzle, a diffuser and a flange were constructed and modeled using a 3D model and ANSYS-FLUENT 6.3. The aim of this modeling study is to get the results for an optimum geometric shape that generates the highest wind velocity in front of the wind turbine installed inside the structure at the position where the air velocity is maximum. In addition, one major aim of the present study is to compare the results of the 3D model in case of the presence of the wind turbine inside the FDAWT structure with the case of empty structure (without the turbine). Moreover, the obtained results for velocity and pressure distributions, within the study domain, for the two 3D cases are compared with the results obtained previously by the present authors using 2D model.

2- Numerical Procedure

The flow around a wind turbine is governed by the Navier-Stokes equations. Unfortunately, these equations are so complex that analytical solutions only have been found for simple cases. Numerical techniques can be used to solve these complex equations, Jonkman [11]. CFD models are based on the incompressible Reynolds-Averaged Navier-Stokes (RANS) equations derived from the main principles of conservation of mass and momentum, Sumner et al. [12].

In ANSYS FLUENT core there are two available numerical methods, applied for several conditions. The first solver is pressure-based solver which mainly used for low-speed incompressible flows although, the second solver designed as density-based solver, were created for application in high-speed flows. In the present study pressure-based approach was applied.

Two-equation models are the most turbulent models used in the CFD history. The main features of k- ϵ models are robustness, the economic submitted in computer terms, and the behavior presented for wide range of turbulent flows generating a reasonable accuracy, FLUENT [13]. The standard form of the k- ϵ turbulence model is originally proposed by Launder and Spalding [14]. The turbulent kinetic energy, k, and its dissipation rate, ϵ , are obtained from the following transport equations:

$$\frac{\partial}{\partial t}(\rho k) + \frac{\partial k}{\partial x_i}(\rho k u_i) = \frac{\partial}{\partial x_j} \left[\left(\mu + \frac{\mu_t}{\sigma_k} \right) \frac{\partial k}{\partial x_j} \right] + G_k + G_b - \rho \epsilon + S_k \quad (2)$$

$$\frac{\partial}{\partial t}(\rho \epsilon) + \frac{\partial \epsilon}{\partial x_i}(\rho \epsilon u_i) = \frac{\partial}{\partial x_j} \left[\left(\mu + \frac{\mu_t}{\sigma_\epsilon} \right) \frac{\partial \epsilon}{\partial x_j} \right] + C_{1\epsilon} \frac{\epsilon}{k} (G_k + C_{3\epsilon} G_b) - C_{2\epsilon} \rho \frac{\epsilon^2}{k} + S_\epsilon \quad (3)$$

In these equations, G_k , shows the production of turbulence kinetic energy due to the average velocity slopes, and is described in Fluent. G_b signs to the turbulence kinetic energy generation due to buoyancy. $C_{1\epsilon}$, $C_{2\epsilon}$ and $C_{3\epsilon}$ are constants, also σ_k and σ_ϵ are turbulent Prandtl numbers for k and ϵ . S_k and S_ϵ are user-defined sources terms. Thereby, this approximation estimation to the turbulence inputs of k- ϵ model is used in the present work.

Figure 2 shows the boundary conditions and outer domain for the flanged diffuser structure, where the Inlet boundary (on the left-hand side border) is set as a velocity Inlet, the outlet boundary (on the right-hand side border) is set as pressure outlet, and the top boundary is set as an open stream while the bottom boundary is set as an axis. The model dimensions have been drawn in reference to the throat diameter D of the flanged diffuser.

In order to ensure the solution convergence, the resulting solution must satisfy the following conditions:

Residual RMS values have been reduced to an acceptable value (typically 10^{-4}). Monitor values of the fields of interest (such as drag, lift and momentum residuals) have to reach a steady solution. These conditions are satisfied in the present study and the details are given in Abdelrazik [9].

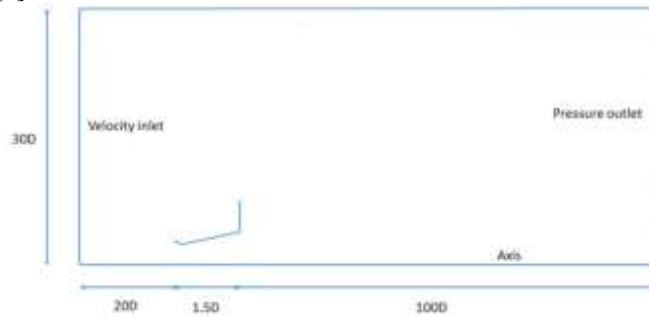


Figure 2 Computational domain and boundary conditions for the flanged diffuser structure

In the present study, in order to ensure the mesh independency of the solution, four different grids are tested to prove that refining and increasing the number of nodes and elements will not have a big effect on the results accuracy. Grid independence study is performed by choosing one point inside the diffuser and tracking the pressure value for the same point in the four different grids. Each grid has number of nodes as shown in Table 1.

Table 1 The number of nodes for the four different grids.

Grid NO.	Number of nodes
1	41,894
2	64,234
3	94,094
4	123,694

As shown in Fig. 3 the pressure value begins (-18.664 pa) then it decreases to about (-21.717pa) and this value can be considered constant from the second to the fourth grid. The third mesh in the grid independence study is used for the flanged diffuser cases, (94,094) nodes are used for the present study to decrease the iterating time.

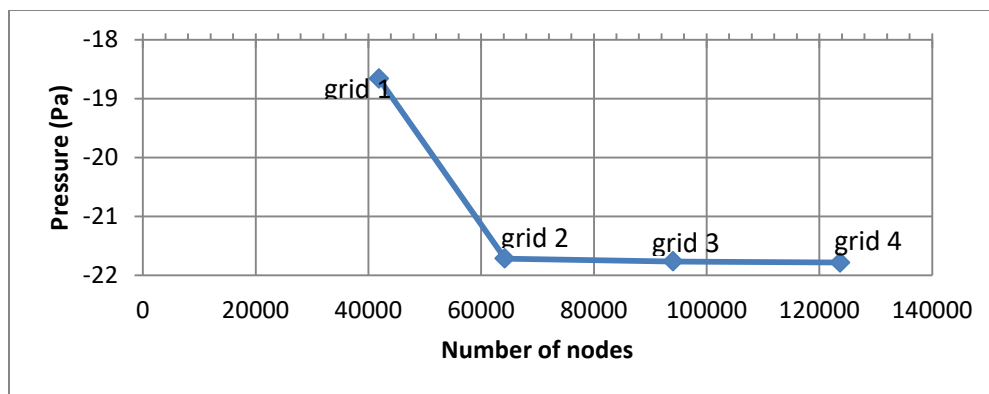


Figure 3 Grid independence curve

A comparison has carried out between experiments that have been performed in order to find out the maximum velocity that could be generated from different geometric shapes such as the nozzle, cylinder and diffuser, Abe et al. [7], and the results obtained in the present study through the Fluent ANSYS software in order to ensure the validity of the criteria used in the present study as shown in Fig. 4. This figure shows that the results from generated simulations are in agreement with the reference ones. Accordingly, the generated model is valid and could be safely developed and optimized.

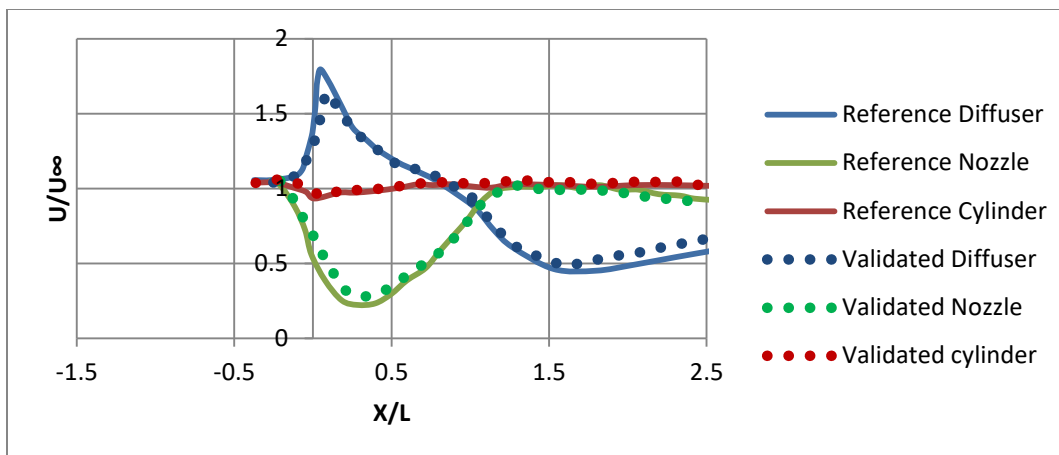


Figure 4 Validation for performed simulation for the wind velocity on the central axis of three different geometric structures i.e. diffuser, nozzle and cylindrical ducts, present study and Abe et al. [7].

3- Results and discussion

The results and discussion related to find the optimum augmented diffuser shape are presented in the present study using 3D approach in comparison to previously obtained 2D results. Nozzle length, nozzle angle, diffuser length, diffuser angle and, flange height, are the parameters that control the performance of the flanged diffuser augmented wind turbine (DAWT).

3-1 The results of the previous 2D modeling studies by the present authors

In previous 2D studies by the present authors, Abdelrazik [9] and Abdelrazek et al. [10], Optimization trials were carried out in a successive form by varying the five parameters dimensions in a dimensionless form. Each trial is studied carefully, in order to find out the best case in each attempt. The best case is selected as per the highest wind speed inside the augmented wind turbine structure at or around the throat, where the wind rotor is placed. It was aimed to reach the optimum structure shape of the augmented diffuser by using design of experiments technique. Thirty random cases are introduced to get the best velocity by using ANSYS-FLUENT 6.3 and the results are implemented in matrix and LU decomposition is used to get the best result. The reachable optimum design dimensions are given in Table 2 and shown in Fig. 5:

Table 5. 1 the optimum shape dimensions, 2D study, Abdelrazik [9]

Nozzle Length	Nozzle angle	Diffuser length	Diffuser angle	Flange height
0.25D	22°	1.45D	12°	0.9D

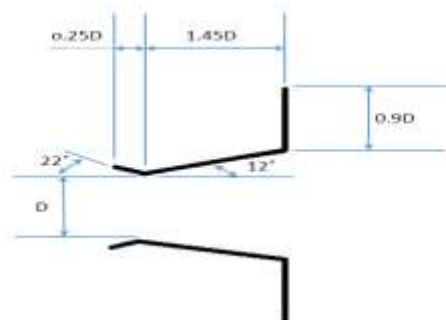


Figure 5 the optimum geometric shape, 2D study, Abdelrazik [9]

The optimum geometry of the flanged diffuser (best case) was restored in order to fit the conditions of Alexandria, Egypt and similar places in the world, where this city preserves an average wind velocity of 5 m/s. This value is considered an input value for the flanged diffuser optimal geometry, in order to know if it is going to be worth to install this assembly in these low velocity places. This will lead to distribute the wind turbines all over the world lands instead of concentrate the wind turbines in the limited places of high wind speeds (more than 8-10 m/s).

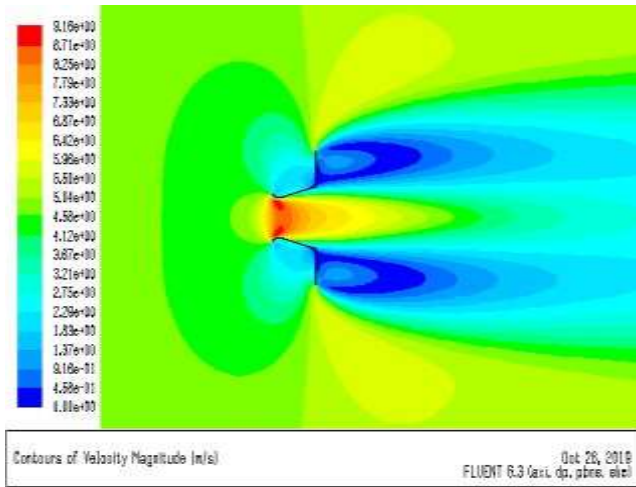


Figure 6 Velocity contours of the optimum shape

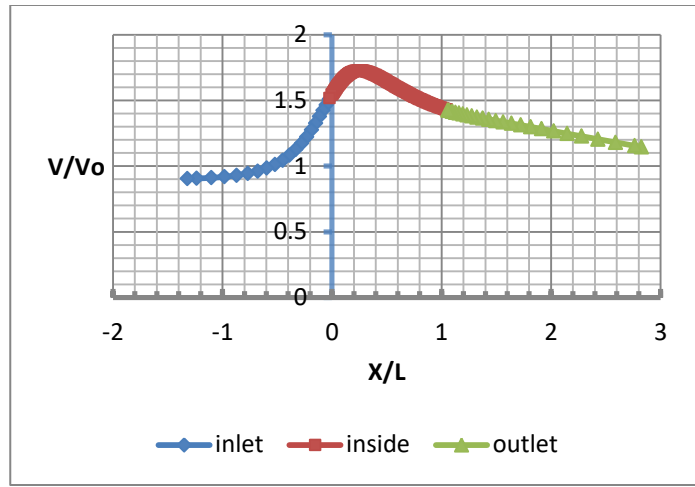


Figure 7 Velocity distribution of the optimum shape

The results shown in Figs. 6 and 7, for the 2D case without the presents of the wind turbine inside the structure, reveal that when the input velocity for the optimum geometry was 5 m/s, the resulting maximum velocity was 8.54 m/s ($\frac{V}{V_0} = 1.71$). This value (8.54 m/s) is considered one of the target velocities values for wind turbines in order to achieve the highest power from wind turbine in the case of low wind speed.

As shown in Fig. 8, for the pressure contours the flanged diffuser played a role to collect and accelerate the wind. The flange generated a low-pressure region in the exit of the diffuser by vortex formation. This leads to draw more mass to the wind turbine inside the diffuser shroud.

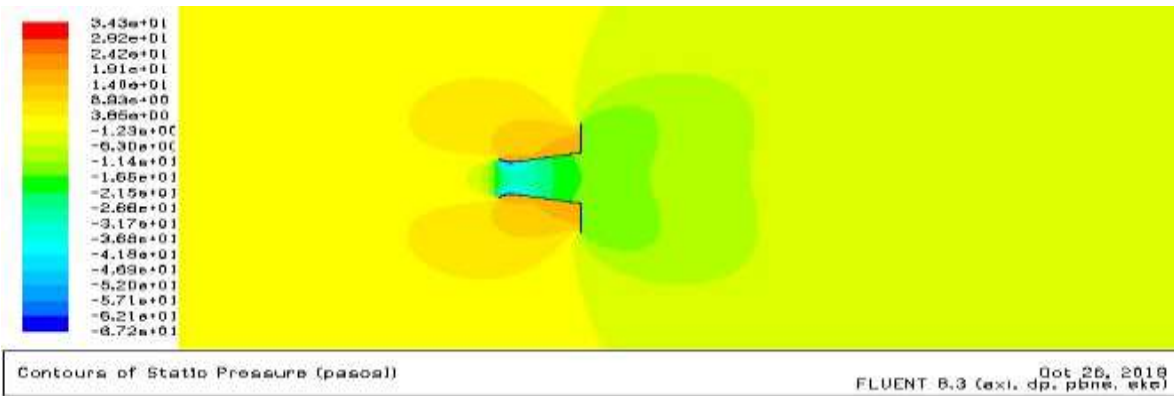


Figure 8 Static pressure contours for the optimum shape

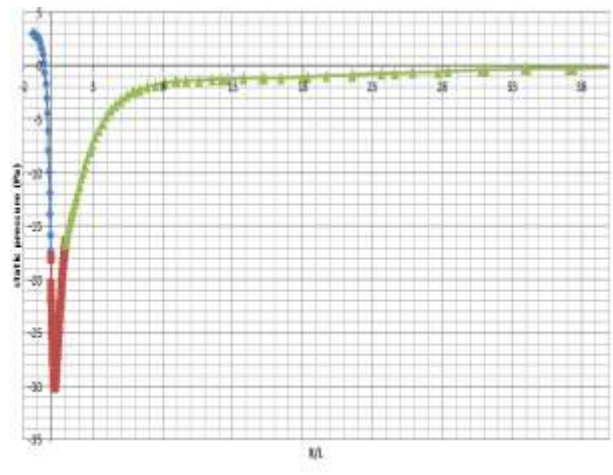
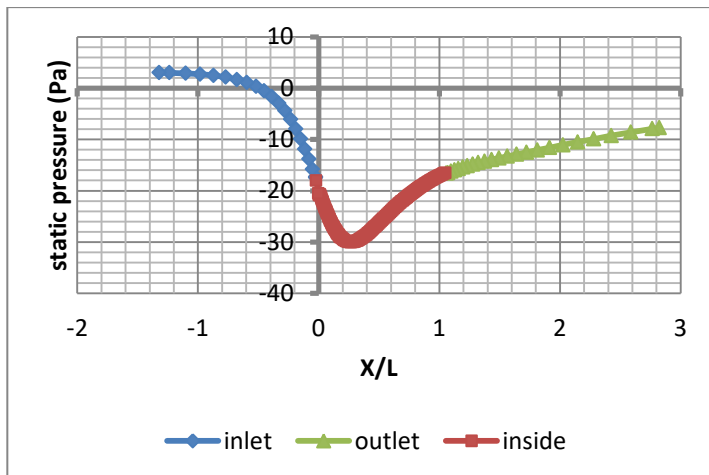


Figure 9 (a) and (b) The optimum shape Static and back pressure distribution

The pressure distribution in Figs. 9 (a, b) illustrate the big role of the diffuser's flange which increased the pressure in front of it, resulting in a pressure drop behind it. This pressure drops served well the wind velocity inside the diffuser, which caused the increase of the wind velocity inside the structure.

In Fig. 9-a, the horizontal axis ended at ($\frac{x}{L} = 3$), while in Fig. 9-b the horizontal axis extended to ($\frac{x}{L} = 38$), to show how the pressure reaches the atmospheric back pressure.

Comparing the output power from FDAWT with maximum velocity 8.54 m/s with the extracted power from bare wind turbine with inlet velocity $V_0 = 5 \frac{m}{s}$, the output power increased by 483%. These results are in agreement with many other researchers, for example [15].

3-2 The effect of inserting a wind turbine inside a flanged diffuser structure

In order to check that the losses caused from the wind turbine when placed inside the flanged diffuser structure are accepted, one of the following two approaches can be performed [8]:

- Creating a three-dimensional, 3D, model for the flanged diffuser and installing the wind turbine inside it.
- Creating a two-dimensional, 2D, model for the flanged diffuser and placing the wind turbine inside it and finding out the load factor for many cases.

The present study selected the 3D option, where this option presents the real case of the wind turbine. The option of the load factor mainly depends on assuming the working hours for the wind turbine, which will produce non-precise results.

3-3 3D Model results before inserting the blades

A 3D model is created to find out the effect of the model dimensions (2 or 3) on the obtained performance results in a flanged diffuser augmented wind turbine structure. In addition, the 3D results will be a base to compare the performance results of the optimal geometry of the FDAWT structure in case of the presence of the turbine rotor inside the structure at the diffuser inlet. The 3D model consists of a cylindrical shaped domain and a flanged diffuser. The present study used a three blades wind turbine. Therefore, a slice of 120° is taken along the axis of the cylindrical shaped domain. The one-third slice is taken in order to reduce the running time and number of iterations performed by the software, as the remaining 240° are similar to the taken 120° slice. Figure 10 shows the built 3D model. The symmetric model helps in saving much more time, noting that the 120° symmetric section is only applicable when a 3-blade wind turbine is used.

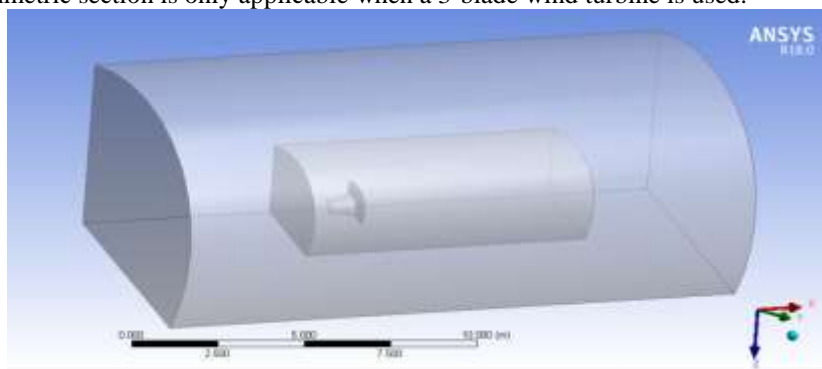


Figure 10 Overall 3D geometry model

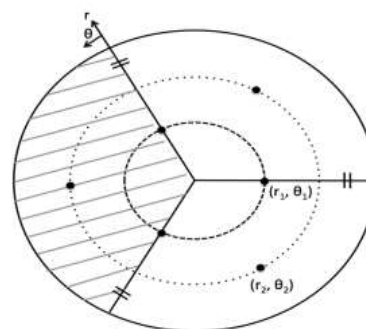


Figure 11 The periodic boundaries

In this case, the velocity distribution at angle θ of 0 and 120 degrees are the same. θ_1 represents one of the periodic boundaries for the $1/3$ domain and θ_2 is the other boundary as displayed in Figure 11.

The next step is applying the mesh model, where this step proves the significance of modeling only a one third slice of the concerned model, while applying a cyclic symmetric model. The mesh density has been concentrated near the flanged diffuser structure, the mesh high density has been considered in these areas as a result of great change of velocity and pressure in these areas, which require increasing the mesh elements in order to have accurate results. In this model 452,852 nodes and 2,592,781 elements are used to define the mesh. The meshing different densities are shown in Figure 12.

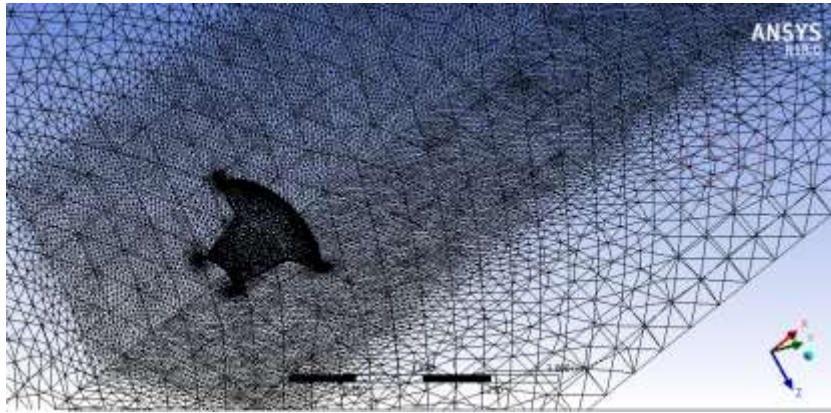


Figure 12 Overall 3D meshing model

A velocity of 5 m/s has been used as an inlet boundary condition for the 3D model, where velocity and pressure contours and distributions have been generated. These results will be compared with the results of the 2D models obtained by the authors (Abdelrazik [9] and Abdelrazek et al. [10]).

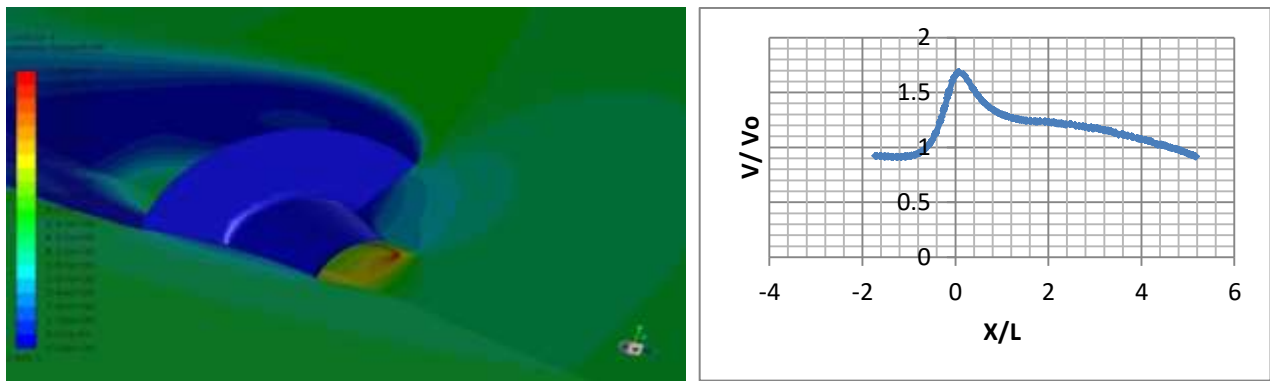


Figure 13 Velocity contours (a) and distribution (b) along the axis of the diffuser for the optimum shape before inserting the blades, 3D results

The velocity and pressure contours and distributions shown in Figs. 13 and 14 clarified the big role of the diffuser's flange in increasing the wind velocity inside the diffuser and decreasing the pressure behind it. This increase in wind velocity was a result of dropping the velocity after the flange as shown. The results for the 3D cases are in agreement with the previous results related to 2D case.

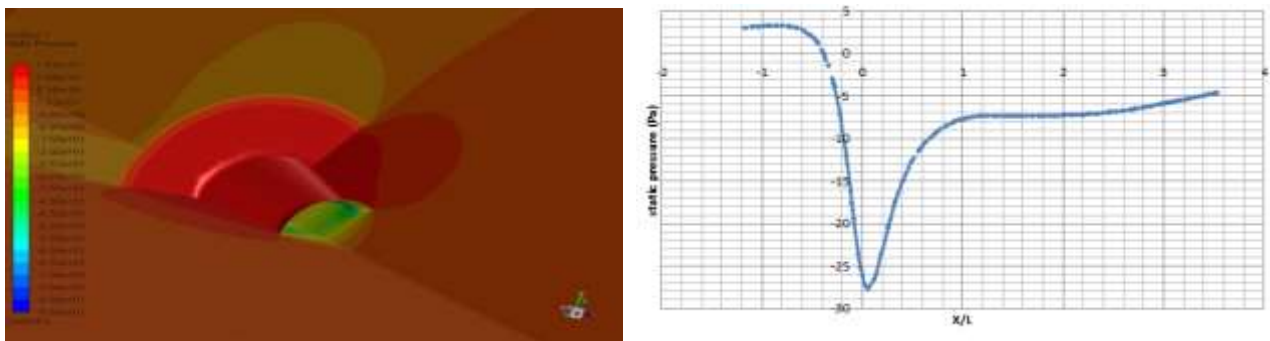


Figure 14 Pressure contours (a) and distribution (b) along the axis of the diffuser for the optimum shape before inserting the blades, 3D results

3-4 After inserting the wind turbine

Wind turbine blades are placed at the diffuser throat, Fig. 15, to find out the effect of placing the turbine inside the FDAWT structure in the wind turbine performance. This will be obtained by comparing the velocity and the pressure results before and after inserting the wind turbine blades.

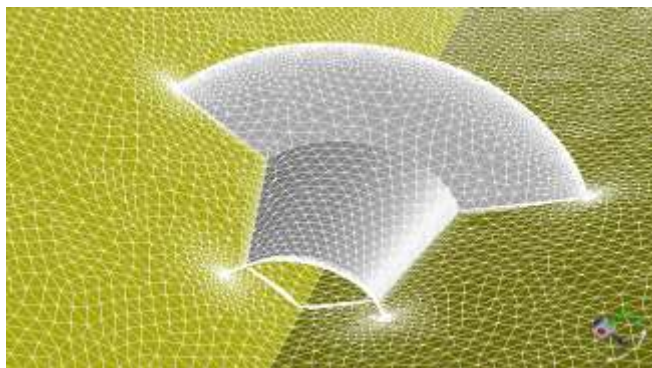


Figure 15 A 3D meshing model of a Wind Turbine Blade inserted in a Flanged Diffuser Structure

As shown in Fig. 16 the maximum dimensionless velocity ratio $\frac{V}{V_0}$ reduced to 1.63 instead of 1.7 for the 3D case without turbine rotor. In addition, Fig. 17, for the pressure distribution shows that the static pressure value at the diffuser throat rose from -28 pa to -25 pa in the case of inserting the wind turbine blades. This happened because some of the wind energy was lost due to the presence of the turbine blades.

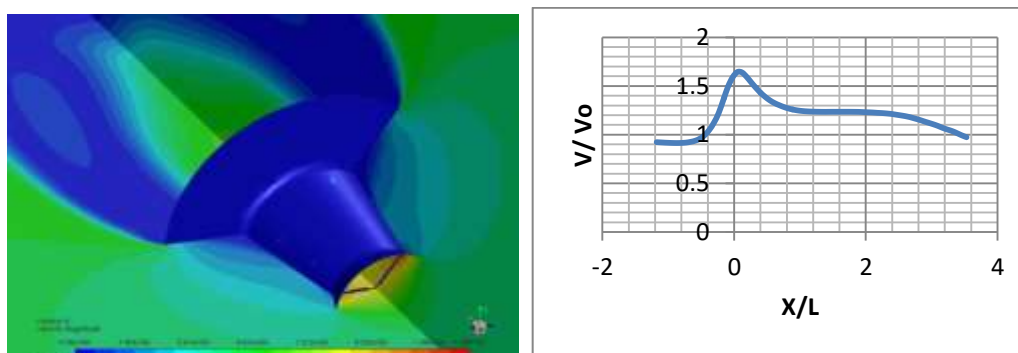


Figure 16 Velocity contours (a) and distribution (b) along the axis of the diffuser for the wind turbine inserted in the optimum Flanged Diffuser Structure

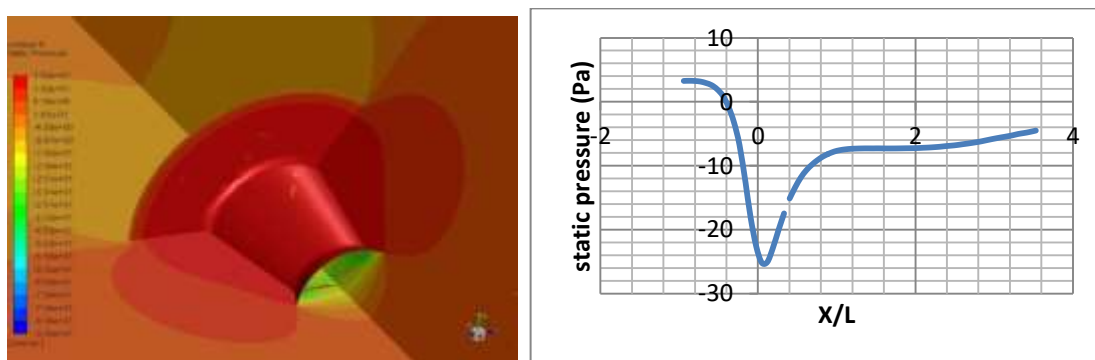


Figure 17 Pressure contours (a) and distribution (b) along the axis of the diffuser for the wind turbine inserted in the optimum Flanged Diffuser Structure

A comparison between the results of the 2D and the 3D results with and without inserting the wind turbine blades is shown in Fig. 18. In the 2D case the wind velocity started to increase at the structure inlet to be $(\frac{V}{V_0} = 1.4)$ and reached its maximum value at the diffuser throat $(\frac{V}{V_0} = 1.71)$ and decreased at the structure outlet in comparison with the 3D case before inserting the blades the velocity ratio decreased to $(\frac{V}{V_0} = 1.7)$ at the diffuser throat but after inserting the blades the velocity ratio decreased to $(\frac{V}{V_0} = 1.63)$ which is the lowest value because some of the wind energy got lost due to the presence of the wind turbine blades in the minimum area inside the structure.

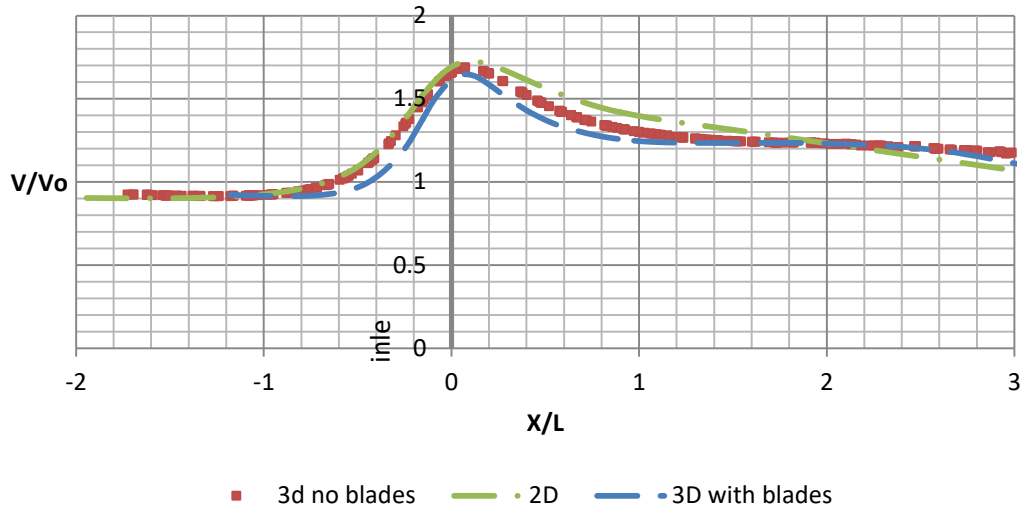


Figure 18 A comparison between the velocity distribution along the axis of the diffuser for the 2D and the 3D models before and after inserting the wind turbine blades

Similarly, it is important to check the pressure distribution curves for the three cases to be sure that it matches the physics. Figure 19 shows that for the 2D case pressure distribution results, it is noticed that the lowest pressure value is $-30 p$ at the diffuser throat. In comparison with the 3D case before inserting the blades the lowest pressure value was $-28 pa$ and after placing the blades the lowest pressure value was $-25 pa$ at the diffuser throat which matches the velocity values. (i.e. lower pressure values, Fig. 19, corresponding to the higher velocity values, Fig. 18, and vice versa). Moreover, Figs. 18 and Figs. 19 show also that there is no change in the trends of the velocity and pressure distributions for the three cases (2D, 3D with and without inserting the turbine).

Finally, it is important to say that, in practice, the wind turbine with its hub and shaft will be presented in front of the wind, beside the wind turbine blades. This will cause a resistance to the flow and creates losses. This means that the effective benefits from the FDAWT structure will be lower than the 63% increase obtained in the present study which considered only the wind turbine blades.

It is also should point out that the previous mentioned effect will be presented in case of the wind turbine placed in open space (i.e., without using the diffuser augmented wind turbine structure), but the resistance in the two cases will not be equal. The case of placing the turbine inside the FDAWT structure will have more resistance than the open domain case due to the blockage effect inside the FDAWT structure at the minimum area where the turbine rotor is placed.

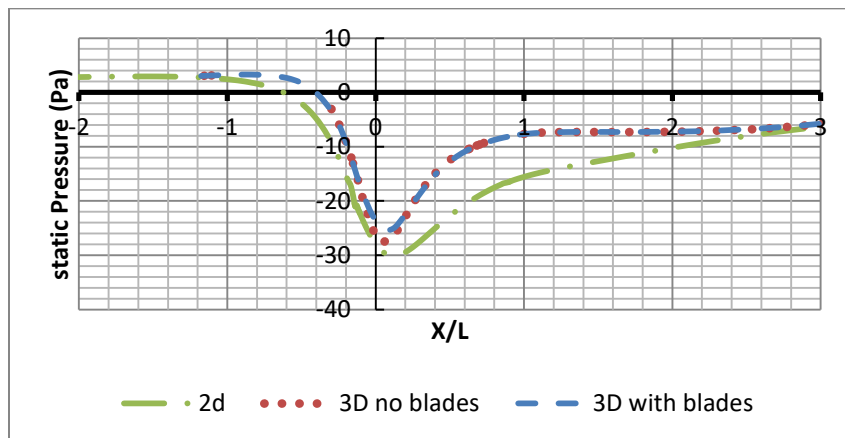


Figure 19 A comparison between the pressure distribution along the axis of the diffuser for the 2D and 3D models after inserting the wind turbine

4- Conclusion

In the present study, a flanged diffuser augmented wind turbine, FDAWT, structure was constructed and modeled using a 3-dimensional, 3D, model using ANSYS-FLUENT 6.3. The aim of this modeling study was to get the results for an optimum geometric shape that generates the highest wind velocity in front of the wind turbine installed inside the structure at the position where the air velocity is maximum. In addition, the present study compared the results of the 3D model in case of the presence of the wind turbine inside FDAWT structure with the case of empty structure (without the turbine). Moreover, the obtained 3D model results for velocity and pressure distributions within the study domain are compared with the results obtained previously by the present authors using 2D model.

The present results obtained using a 3D model reveals that: The velocity ratio of the maximum air velocity along the structure axis, V_{\max} , and the wind velocity, V_0 , V_{\max}/V_0 reached 1.7 (70% increase) before inserting the blades and decreased to $V_{\max}/V_0 = 1.63$ (63% increase) after inserting the blades, compared to $V_{\max}/V_0 = 1.71$ (71% increase) for the case of 2D modeling obtained by the present authors in previous studies.

References

- 1- Olivieri, D., "Design and Testing of a Concentrator Wind Turbine", PhD thesis, The Open University, U.K, 1991.
- 2- De Vries, O., "Fluid Dynamic Aspects of Wind Energy Conversion", AGARDograph No. 243, 1979.
- 3- Ohya, Y., Karasudani, T. and Sakurai, A., "Development of a Shrouded Wind Turbine with a Flanged Diffuser", Journal of Wind Engineering and Industrial Aerodynamics, Vol. 96, pp. 524-539, 2008.
- 4- Sarwar, M., Nawshin, N. and Imam, M., "A New Approach to Improve the Performance of an Existing Small Wind Turbine by using Diffuser", International Journal of Engineering & Applied Science, Vol. 4, pp. 31- 42, 2012.
- 5- Jafari, S., and Kosasih, B., "Flow Analysis of Shrouded Small Wind Turbine with a Simple Frustum Diffuser with Computational Fluid Dynamics Simulations", Journal of Wind Energy, pp.102-110, 2014.
- 6- Hjort, S., and Larsen, H., "A Multi-Element Diffuser Augmented Wind Turbine", Energies, pp.3256-3281, 2014.
- 7- Abe, K., Nishida, M., Sakurai, A., and Ohya, Y., "Experimental and Numerical Investigations of Flow Fields behind a Small Wind Turbine with a Flanged Diffuser", Journal of Wind Engineering and Industrial Aerodynamics, Vol.93, pp. 951-970, 2005.
- 8- Abdulaziz, A., "Study of the Performance of a Flanged Diffuser Augmented Wind Turbine", M. Sc. Thesis, Alexandria University, Egypt, 2017.
- 9- Abdelrazik, A. M., "Optimization of a diffuser augmented wind turbine structure performance using design of experiments technique", M. Sc. Thesis, Alexandria University, Egypt, 2021.
- 10- Abdelrazek, A. M., Abdelrazik, A. M., and Kassab, S. Z., "Performance of a flanged diffuser augmented wind turbine structure under variable geometrical conditions", The 2nd International Conference on Engineering Science and Technology (ICET 2021), Luxor, Egypt, February 3-4, 2021, Accepted.
- 11- Jonkman, J. M., "Modeling of the UAE wind turbine for refinement FAST-AD, Technical Report", National Renewable Energy Laboratory, 2003.
- 12- Sumner, J., Wattersl S., and Masson, C., "CFD in wind energy: The virtual, multiscale wind tunnel", Energies, pp. 989–1013, 2010.
- 13- Fluent, ANSYS FLUENT 14.0 Documentation, ANSYS, Inc., 2011.
- 14- Launder, E., and Spalding. B., "Lectures in Mathematical Models of Turbulence", Academic Press, London, England, 1972.
- 15- Kulkarni, S. and Badhe, A., "Experimental Validation of Computational Design of Wind Turbine with Wind Lens", International Journal of Mechanical Engineering, pp. 9-13, 2019.